STUDY OF THE STIFFNESS FUNCTION IN THE SPUR GEAR CONTACT USING THE FINITE ELEMENT METHOD

Roman Savonov roman@ita.br
João Carlos Menezes menezes@mec.ita.br
Instituto Tecnológico de Aeronáutica - ITA
Div. de Eng. Mecânica - Aeronáutica, 12228-900, São José dos Campos - SP – Brazil

Abstract: *The aim of this work is to study of the stiffness of the teeth of a pair of gears, concerning the dynamical response of mechanical system. This contact is named Hertz contact and occurs at contact of two solids one of witch has curved surfaces. The surfaces are cylindrical in case of contact of two teeth of gears. The curvature radius of the curve is not permanent. It changes at every point of the profile. It is described by an evolvent function. The Finite Elements software "FEMAP 8.3" was used to derive the torque-θ function. These results were applied in the solution of the dynamical problem of two flexible axes with a pair of gears. Details of the finite element model of the gear teeth are presented. Information from this model were used to estimate the teeth's stiffness, and, at last, included in the matrix equation of motion of the system.*

***Keywords**: Hertz contact, spur gears, Finite Element*

1. INTRODUCTION

The transmission by gear mechanisms is very used in several fields of industry. The greater number of the machines has gear transmission. Therefore, its optimization is necessary to improve a quality and durability of mechanisms. The study of the teeth contact and dynamics of transmission is very important to make these properties better.

The evaluation of gear teeth contact is complicated by its nonlinear nature. The contact of this type is named Hertz contact and occurs at contact of two solids one of witch has curved surfaces. The first proceeding discussing this theme was done and published in 1950 (Poritsky, 1950).The author presented in his work the equations of the stress' behavior due to applied forces. Several types of Hertz contact such as rolling and sliding contact were analyzed, and their applications were presented. For example, the rolling contact under normal load occurs in rail wheels, and, under normal and tangential load in locomotive driving wheels, and in braked rail wheels. In contact of gear teeth, rolling contact occurs at the pitch point, elsewhere contact is of the sliding variety.

Later, with development of industry, the mathematical models for dynamic analysis of gears became necessary. During decades, many models for mathematical resolution were developed. Özgüven and Houzer (1988) revised several publications and analyzed the existent models. They divided the models into five principal classes and showed witch type of models are involved into each class, and for witch case each model was used more adequately. The authors explained the basic principles of each class of models, their advantages and disadvantages.

A six-degree-of-freedom nonlinear semi-definite model with time varying mesh stiffness has been developed for dynamic analysis of spur gears by Özgüven (1990). The model includes a spur gear pair, two inertias representing load and prime mover, and bearing. The software employs digital simulation technique for the solution, and is capable of calculating dynamic tooth and mesh forces, dynamic factors for pinion and gear, dynamic transmission error, dynamic bearing forces and torsions of shafts.

With the development of more efficient machines, more powerful computers stimulated the solution of more complex and sophistic problems. Andersson and Vedmar (2002) presented a method to determine the dynamic load between two rotation elastic helical gears. The stiffness of gear teeth was calculated by the finite element method and includes the contribution from the elliptic distributed tooth load. A numerical example was presented with results that show the behavior of the dynamic transmission error, as well as, the variation of the contact due to the dynamic load for different rotation speeds. Tao Sun and HaiYan Hu (2003) presented the study of more complex problems. The non-linear dynamic of a planetary gear system with multiple clearances was analyzed. The solution was determined by using harmonic balance method. The theoretical result has been verified by using the numerical integration.

The finite element analysis is most popular in last decade due to its most exact results in comparison to other methods. Several problems such as static, dynamic, structural and vibration problems can be solved using this method. The finite element model of the teeth contact, application of the boundary conditions, description of finite element analysis using the software "FEMAP 8.3" and figures of the result are presented in this paper.

2. THE FINITE ELEMENT ANALYSIS USING SOFTWARE "FEMAP 8.3"

2.1. The formulation of the problem

The derivation of the stiffness function for application in the dynamical analysis of the gear transmission is discussed. A simple example of the dynamical system, where the stiffness function of the gear has been applied, is shown in Fig.1. The stiffness function of the gear is presented as stiffness of the spring ($k(\Delta\theta)$).

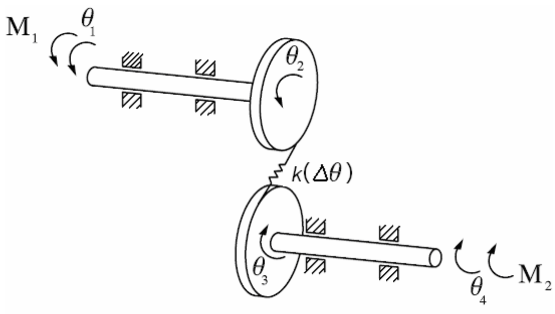

Figure 1. A example of a dynamical system.

The geometrical properties of the analyzed involute spur gears are shown in the Tab.1.

Table 1. Geometrical properties of the spur gear.

DESCRIPTION	GEAR
Number of the teeth, *z(mm)*	25
Module, *m(mm)*	2
Pitch diameter, d_p	50
Diametral pitch, *P*	6,28
Addendum diameter , d_e	54
Dedendum diameter, d_i	45
Pressure angle, α	20
Base diameter, d_b	46,98
Addendum, *a*	2
Addendum (cordal), a_c	2,049
Dedendum, *b*	2,334
Tooth height, *h*	4,334
Tooth angle, θ	3,6

The tooth's profile has been generated in accordance to a method introduced by Litvin (NASA) or Belokonev (1985), and is illustrated in Fig. 2.

Figure 2. The profile of the tooth.

The stiffness of the tooth varies in each point of the profile due the variation of the curvature radius. Therefore, the tooth's profile is divided into five parts, according to Fig.2. It is considered that the radius of the tooth's curvature is constant inside each part, and varies from one to each other part. Each of the tooth's part has a suitable stiffness function. The teeth are symmetric and three cases of teeth's contact correspond to five divisions of the tooth as presented in Fig.3.

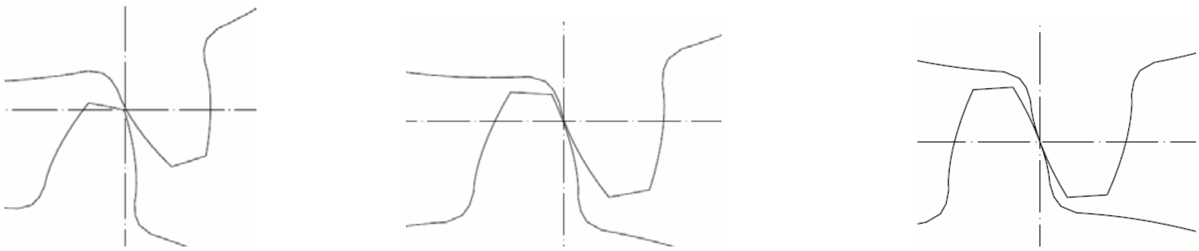

(a) (b) (c)

Figure 3. Three cases of teeth contact: a) initial contact; b) intermediary contact; c) base circle contact.

The first case of contact (Fig.1 (a)) corresponds to parts 1 and 5 (Fig.1), the second case (Fig.2 (b)) corresponds to parts 2 and 4, and case 3 (Fig.2 (c)) corresponds to part 3. Finite element models have been created for each of these cases, in order to determine the stiffness function. The mechanical properties of the teeth' material are presented in Tab.2.

Table 2. Mechanical properties of the teeth' material.

Properties	valor
Density, ρ (kg/m^3)	7800
Youngs Modulus, E(kg/cm^2)	2,1x10^6
Compress Strength (kg/cm^2)	2800
Tension Strength (kg/cm^2)	4600
Shear Strength (kg/cm^2)	3600
Poisson's Ratio	0,3

2.2. Aplication of boundary conditions

Finite element models were created for each of the three cases. The 2D tooth's geometry was created employing the software "AutoCAD 2006" and then imported to "FEMAP 8.3" for analysis. The technique to make the mesh of the finite element is similar; therefore, only one of the three cases is described.

The tooth is subjected to lager stresses due to local contact, and, for that reason, has a more refined mesh than the cylindrical body of the gear. First, the profile of gear is divided into bi-dimensional finite elements, and, after that, the mesh is extruded along the x axis, according to Fig. 3.

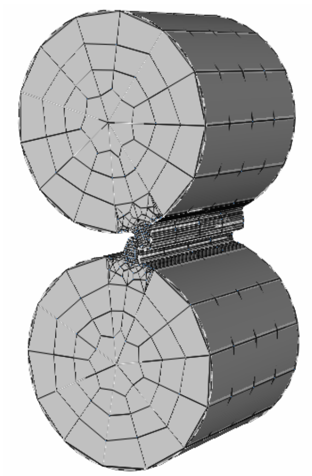

Figure 3. Finite element model of the gear.

The element "slide line" is used to warrant the contact between two gears. This element has several options, witch should be adopted in accordance to each particular case of analysis. It is shown in Fig.4.

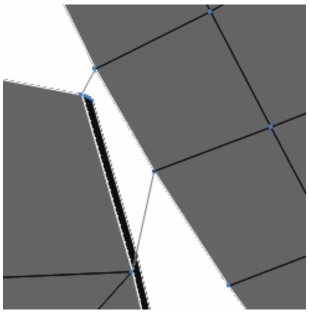

Figure 4. The element of the contact "slide line".

The distribution of stresses due to Hertz contact is non-linear. "FEMAP 8.3" has a particular mode for this type of problem. The analyzed model with application of boundary conditions is presented in Fig. 5.

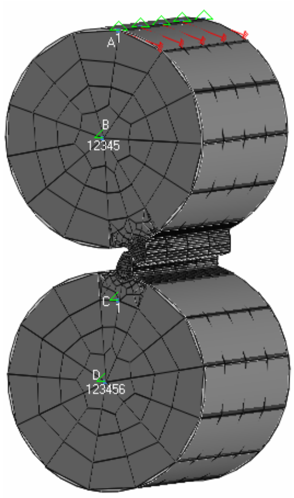

Figure 5. Finite element model of gear with application of boundary conditions.

The "forced dislocation" is used in the nonlinear mode of analysis as force applied to model. These forces are dispersed uniformly along the axis of cylindrical part of the gear in point *A* as shows the Fig.5. The green triangles in projection of point *A* are restrictions, but in this case, its serves as connection of the "forced dislocations" with the body of gear. The direction of the force is tangential to the circumference; in witch the point *A* is situated. It is done to simplify the conversion of the "forced dislocations" to rotation displacement. The five degrees of freedom are restricted in point *B*, Fig.5, and, in its projections uniformly distributed along the cylindrical part axis of the gear, alike the forces in point *A*. Therefore, rotation around gear axis is free. Displacements along the x axis is restricted in point *C*. All degrees of freedom are restricted in point *D*, the central point of lower gear, according to Fig.5. All these operations with model were executed for the sake of simplify of interpretation of the analysis results and, also, to allow the derivation of the relation of the torque applied to gear as function of the gear rotation.

After application of boundary conditions, the model is ready for analysis.

2.3. Analysis results.

Nonlinear analysis has two options. It may be done with symmetrical and nonsymmetrical penetration. The analysis option "symmetrical penetration" requires less time, but the results are obtained for the "slave" part only (gear in the top). The analysis with nonsymmetrical penetration with forty iterations has been done in this case. The resulting stress distribution for three cases are showen in Figs.5,6,7.

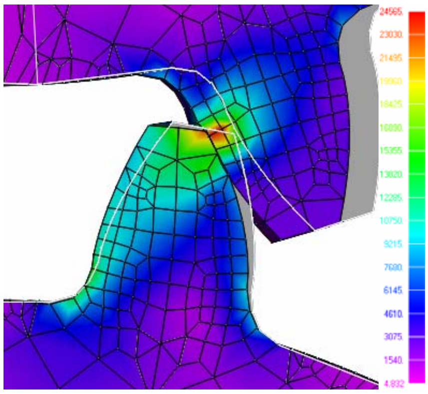

Figure 5. Stress distribution for the first case.

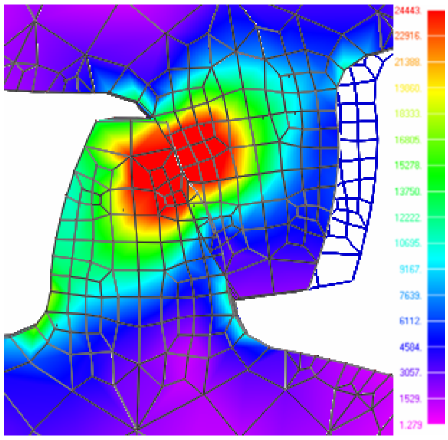

Figure 6. Stress distribution for the second case.

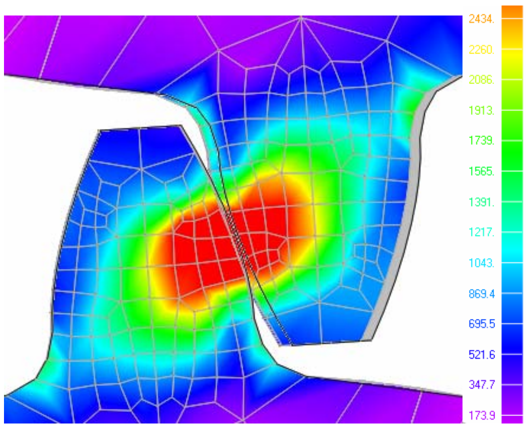

Figure 7. Stress distribution for the third case .

The data of the restriction force in point *C* and the displacements in point *A*, according to Fig.5, are obtained in *FEMAP 8.3* and then imported to *Excel*. Torque T_x is obtained by multiplication of the restriction force by radius *CD*, and, the rotation θ by multiplying the displacement *x* by radius *BA*. The new data (T_x - θ) is interpolated by a second degree polynomial. The obtained data for the three cases is presented in Tabs.3, 4 and 5. The interpolation curves are presented in Fig.8.

Table 3. Obtained data for the first case of contact.

Force Fx(N)	Displacement x(mm)	Torque Tx(N*m)	Forced displacement x(mm)	Rotation θ(rad)
0	0,068455	0	0	0
272,983	0,091266	4,5588161	0,022811	0,001013822
984,169	0,13689	16,4356223	0,068435	0,003041556
1697,62	0,18253	28,350254	0,114075	0,00507
2412,88	0,22819	40,295096	0,159735	0,007099333
3128,39	0,27386	52,244113	0,205405	0,009129111
3920,01	0,31956	65,464167	0,251105	0,011160222
4658,42	0,36526	77,795614	0,296805	0,013191333
5499,8	0,41097	91,84666	0,342515	0,015222889
6340,66	0,45669	105,889022	0,388235	0,017254889
7180,7	0,50243	119,91769	0,433975	0,019287778
8020,13	0,54818	133,936171	0,479725	0,021321111
8859,53	0,59395	147,954151	0,525495	0,023355333
9698,54	0,63974	161,965618	0,571285	0,025390444
10538	0,68554	175,9846	0,617085	0,027426

Table 4. Obtained data for the second case of contact

Force Fx(N)	Displacement x(mm)	Torque Tx(N*m)	Forced displacement x(mm)	Rotation θ(rad)
0	0,023717	0	0	0
20,4525	0,047434	0,346833495	0,023717	0,001054089
154,12	0,094868	2,61356696	0,071151	0,003162267
340,476	0,1423	5,773792008	0,118583	0,005270356
526,155	0,18974	8,92253649	0,166023	0,0073788
710,744	0,23717	12,05279675	0,213453	0,0094868
894,193	0,2846	15,16372489	0,260883	0,0115948
1076,44	0,33204	18,25426952	0,308323	0,013703244
1257,46	0,37947	21,32400668	0,355753	0,015811244
1437,35	0,42691	24,3745813	0,403193	0,017919689
1616,14	0,47434	27,40650212	0,450623	0,020027689
1793,54	0,52178	30,41485132	0,498063	0,022136133
1968,84	0,56921	33,38758872	0,545493	0,024244133
2141,41	0,61664	36,31403078	0,592923	0,026352133
2311,38	0,66408	39,19638204	0,640363	0,028460578
2478,34	0,71151	42,02768972	0,687793	0,030568578

Table 5. Obtained data for the third case of contact.

Force Fx(N)	Displacement x(mm)	Torque Tx(N*m)	Forced displacement x(mm)	Rotation θ (rad)
0	0,045	0	0	0
20,672	0,05	0,2418624	0,005	0,000222222
114,7	0,065	1,34199	0,02	0,000888889
209,521	0,08	2,4513957	0,035	0,001555556
305,031	0,095	3,5688627	0,05	0,002222222
387,048	0,105	4,5284616	0,06	0,002666667
511,076	0,12	5,9795892	0,075	0,003333333
635,065	0,135	7,4302605	0,09	0,004
759,005	0,15	8,8803585	0,105	0,004666667
882,867	0,165	10,3295439	0,12	0,005333333
1047,9	0,185	12,26043	0,14	0,006222222
1171,53	0,2	13,706901	0,155	0,006888889

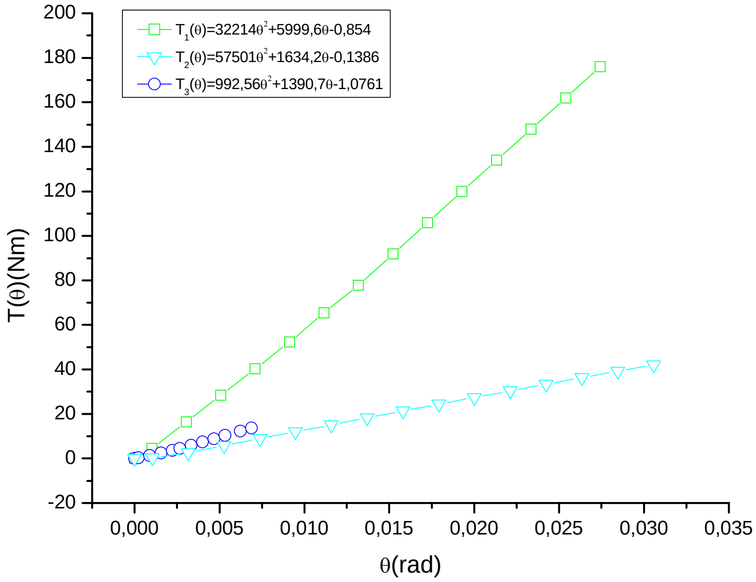

Figure 8. Torque function T_x versus rotation θ

The stiffness function can be obtained by deriving the force function with respect to *x*.

$$k = \frac{\partial F}{\partial x} \tag{1}$$

It is necessary to know the tooth stiffness as a function of rotation for the purpose of dynamical analysis of the system presented in Fig.1. Therefore, Eq.1 must be modified.

$$F = \frac{T(\theta)}{r} \tag{2}$$

$$x = \theta \cdot R \tag{3}$$

Replacing Eqs. 2 and 3 in Eq.1, one obtains

$$k = \frac{\partial(\frac{T}{r})}{\partial(\theta \cdot R)} = \frac{1}{r \cdot R}\frac{\partial T}{\partial \theta} \tag{4}$$

where - T is torque function due θ obtained by FEM using "FEMAP8.3";
θ is rotation;
F is restriction force in the point A;
x is the forced displacement in the point A;
R is the radius of the cylindrical part of the gear equal AB;
r is the distance from rotation axis to the position of application of force F, equal to CD;

The dynamical equation of motion of the system presented in the Fig.1 is:

$$m \cdot \ddot{\theta} + k(\theta) \cdot \theta = T \tag{5}$$

where – m is mass of the system;
$\ddot{\theta}$ is angular acceleration;

θ is rotation;
T is torque;
$k(\theta)$ is stiffness of the tooth;

The function $k(\theta)$ in Eq. 5 is be calculated as an average function. In this case:

$$k = \frac{1}{r \cdot R}\frac{\partial (T_1 + T_2 + T_3)}{\partial \theta} = \frac{1}{r \cdot R}\left(60471{,}8 \cdot \theta + 3008{,}17\right) \tag{6}$$

where $T_1(\theta) = 32214\theta^2 + 5999{,}6\theta - 0{,}854$,

$T_2(\theta) = 992{,}56\theta^2 + 1390{,}7\theta - 1{,}0761$,

$T_3(\theta) = 57501\theta^2 + 1634{,}2\theta - 0{,}1386$

The more exact analysis might be done using three stiffness functions for each fragment of the teeth contact. The involute profile has crescent radius of curvature, thus, each segment of the contact has one determined dominion of the radius. The stiffness $k_1(\theta)$ must be applied for radiuses less than r_1, $k_2(\theta)$ serves for radiuses higher than r_1 and less than r_2, and, $k_3(\theta)$ for radiuses values between r_2 and r_3 as presents in the Fig. 9.

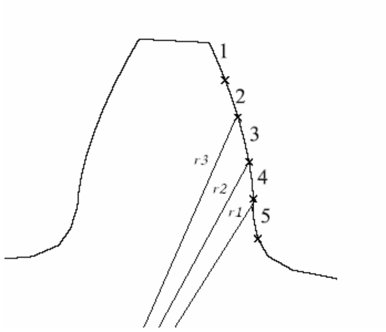

Figure 9. The tooth divided in segment with correspondent radiuses

The process for calculation of radius in the contact point has been proposed by Pimsarn and Kazerounian (2002).

2.4. Conclusions

This work presents the application of a finite element analysis used to determine the stiffness function of the gear teeth contact using the FEMAP 8.3. The obtained stiffness functions were used in dynamical analysis of the gear transmission system involving two flexible axes coupled with pair of spur gear, as shown in the Fig.1. The code for dynamical solution of this mechanical system was done using software Mathematica 5. This problem was solved using the finite element method. The equations of motion were obtained by Lagrange equations. The Newmark method was applied to solve the differential equations. All this factors must be included to the code. Therefore, a combination of solutions method (determination of stiffness function is done by software FEMAP and dynamical analyses of mechanical system evaluate by code in Mathematica) is adequate to improve efficiency and correctness of this type of analysis.

3. ACKNOWLEDGEMENTS

The author wish to thank the financial support of the National Research Committee – CNPq.

4. REFERENCES

Andersson, A., Vedmar, L., “A dynamic Model to Determine Vibrations in Involute Helical Gears”, Journal of Sound and Vibration, Vol. 260, 195-212, 2003
Belokonev, “Theory of Mechanisms and Machines “, Moscow, 1985
F.L. Litvin , Theory of Gearing, NASA Reference Publication 1212.

Ozguven, H. N., Houser, D.R., "Mathematical Models Used in Gear Dynamics - A Review", Jornal of Sound and Vibration, Vol. 121(3), 383-411, 1988

Ozguven, H. N., "A Non-Linear Mathematical Model for Dynamic Analysis of Spur Gears Including Shaft and Bearing Dynamics", Journal of Sound and Vibration, Vol. 145(2), 239-260, 1990

Pimsarn M., Kazerounian K., "Efficient evaluation of spur gear tooth mesh load using pseudo-interference stiffness estimation method", Mechanism and Machine Theory 37 (2002) 769–786, 2002

Poritsky, H., Schenectady, N.Y., "Stresses and Deflections of Cylindrical Bodies in Contact With Application to Contact of Gear and of Locomotive Wheels", Journalof Applied Mechanics,Vol.17(2),191-201,1950

Tao, S., Haiyan, H., "Nonlinear Dynamics of Planetary Gear System with Multiple Clearences", Mechanism and Machine Theory, Vol. 38, 1371-1390, 2003

5. RESPONSIBILITY NOTICE

The authors are the only responsible for the printed material included in this paper.